



Crustal structure of the southern margin of the African continent: Results from geophysical experiments

J. Stankiewicz,¹ N. Parsieglä,² T. Ryberg,¹ K. Gohl,² U. Weckmann,¹ R. Trumbull,¹ and M. Weber¹

Received 31 January 2008; revised 16 July 2008; accepted 1 August 2008; published 21 October 2008.

[1] A number of geophysical onshore and offshore experiments were carried out along a profile across the southern margin of the African Plate in the framework of the Inkaba yeAfrica project. Refraction seismic experiments show that Moho depth decreases rapidly from over 40 km inland to around 30 km at the present coast before gently thinning out toward the Agulhas-Falkland Fracture Zone, which marks the transition zone between the continental and oceanic crust. In the region of the abruptly decreasing Moho depth, in the vicinity of the boundary between the Namaqua-Natal Mobile Belt and the Cape Fold Belt, lower crustal P-wave velocities up to 7.4 km/s are observed. This is interpreted as metabasic lithologies of Precambrian age in the Namaqua-Natal Mobile Belt, or mafic intrusions added to the base of the crust by younger magmatism. The velocity model for the upper crust has excellent resolution and is consistent with the known geological record. A joint interpretation of the velocity model with an electrical conductivity model, obtained from magnetotelluric studies, makes it possible to correlate a high-velocity anomaly north of the center of the Beattie magnetic anomaly with a highly resistive body.

Citation: Stankiewicz, J., N. Parsieglä, T. Ryberg, K. Gohl, U. Weckmann, R. Trumbull, and M. Weber (2008), Crustal structure of the southern margin of the African continent: Results from geophysical experiments, *J. Geophys. Res.*, 113, B10313, doi:10.1029/2008JB005612.

1. Introduction

[2] A number of features make southern Africa a key site for integrated geophysical and geological research on continental accretion and break-up. Bounded to the south by the Agulhas-Falkland Fracture Zone (AFFZ, Figure 1), this region represents one of the world's best examples of a sheared continental margin which formed during break-up of Western Gondwana from about 130 Ma [Ben-Avraham *et al.*, 1997]. At the same time, a classic volcanic rifted margin was developing at the western margin of South Africa. The deep crustal structures and physical properties on these two contrasting margin types, and the nature of the continent-ocean transition across them, are key to understanding the processes of continental break-up and passive margin development. The southern margin of Africa is also of great interest because progressively older crustal provinces are crossed as one moves inboard from the coast (Cape Fold Belt, Namaqua-Natal Mobile Belt, Kaapvaal Craton). The boundaries between these crustal provinces are first-order features relating to continental assembly and information on their 3-D geometry is largely lacking. Particularly important in this respect are the Beattie magnetic anomaly and the Southern Cape Conductivity Belt (Figure 1), which run

roughly parallel to the boundary of the Cape Fold Belt and Namaqua-Natal Belt, and are among the largest and strongest geophysical anomalies on the African continent. Despite the nearly 100 years since their discovery, the geologic nature of these anomalies is still a mystery. Finally, and superimposed on the crustal mosaic, is the huge and economically important Karoo sedimentary basin of Triassic to Jurassic age and the associated lavas and sills of the Karoo Large Igneous Province (LIP) of about 175–185 Ma age.

[3] All of these aspects are addressed in a coordinated program of marine and terrestrial geophysical experiments that has been carried out along the so-called Agulhas-Karoo Geoscience Transect extending from the Agulhas Plateau across the sheared margin and inland as far as the Kaapvaal Craton border (Figure 1). Beginning in 2004, this work has been one of the main research targets of the Inkaba yeAfrica project [de Wit and Horsfield, 2006]. Seismic experiments included wide angle refraction [Stankiewicz *et al.*, 2007], and near-vertical reflection [Lindeque *et al.*, 2007] surveys across the Cape Fold Belt and into the Karoo Basin, magnetotelluric profiles (partially coincident with the seismic survey) across the Beattie Anomaly and Cape Conductivity Belt [Branch *et al.*, 2007; Weckmann *et al.*, 2007a, 2007b], and offshore refraction and reflection seismics [Parsieglä *et al.*, 2007, 2008]. This paper combines and jointly interprets these different data sets along the Western Karoo-Agulhas Profile.

2. Profile Setting

[4] The northern part of the profile runs through the Karoo Basin (KB, Figure 1). This retroarc foreland basin

¹GeoForschungsZentrum Potsdam, Section 2.2 (Deep Geophysical Sounding), Potsdam, Brandenburg, Germany.

²Alfred Wegener Institute for Polar and Marine Research, Bremerhaven, Germany.

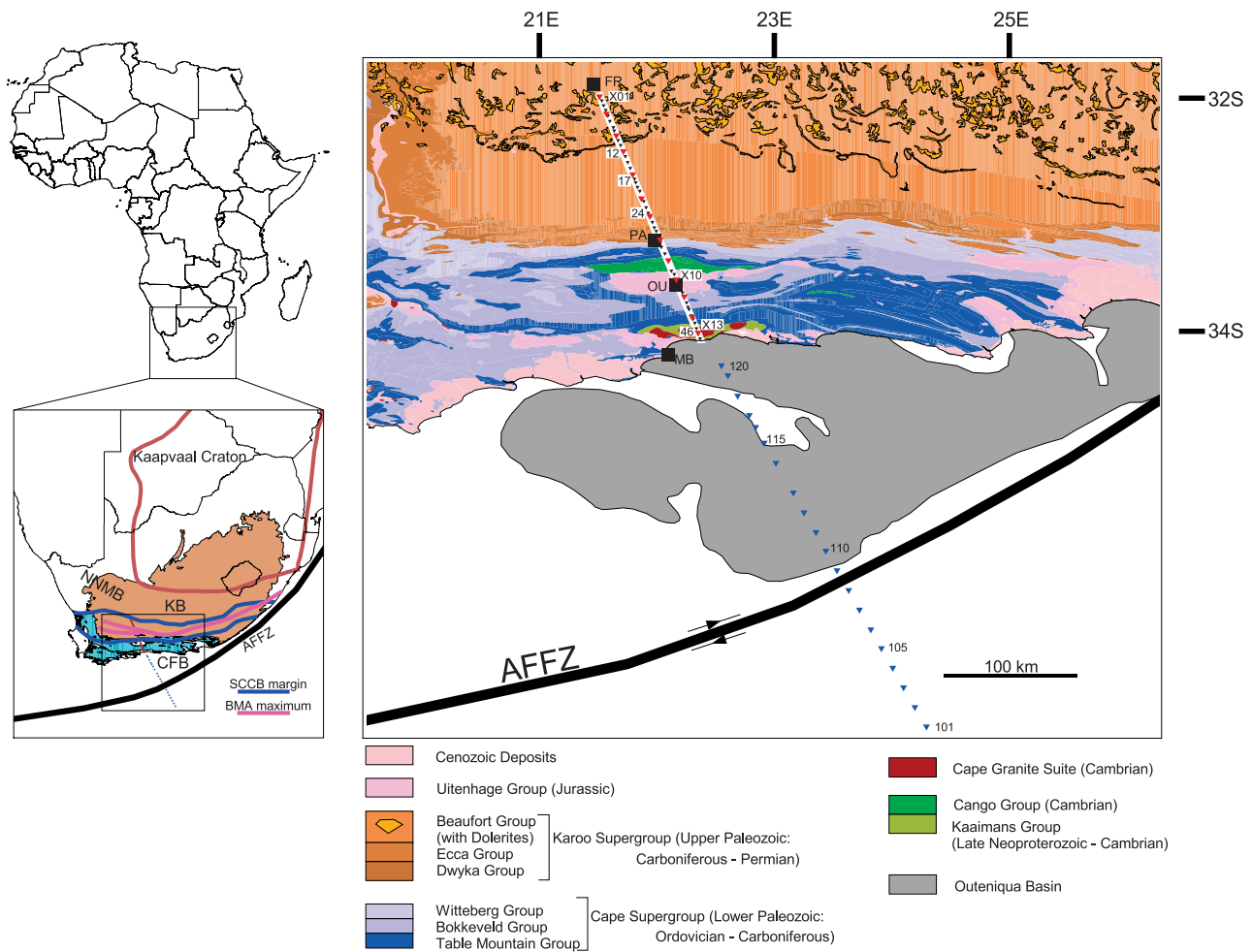


Figure 1. Study area: map of southern Africa showing the relevant large-scale features, like the Kaapvaal Craton, Karoo Basin (KB), Cape Fold Belt (CFB), the location of the Namaqua Natal Mobile Belt (NNMB), the Agulhas-Falkland Fracture Zone (AFFZ), as well the Southern Cape Conductivity Belt and the Beattie magnetic anomaly. The detailed map shows the geological setting of the study area. The onshore section of the profile is indicated by the red triangles (13 shots, numbered X01–X13) and smaller black triangles (48 receivers, numbered 01–48). Four cities are shown on the map to aid the location: Fraserburg (FR), Prince Albert (PA), Oudtshoorn (OU), and Mossel Bay (MB). The 20 ocean bottom seismometers used in the offshore part are marked as blue triangles and are numbered 101–120 following the notation of *Parsieglä et al.* [2007].

is believed to have formed during the accretion of the paleo-Pacific plate to the Gondwana plate during the Late Carboniferous [Cole, 1992]. The basin contains up to 12 km of Late Carboniferous to Mid Jurassic sedimentary strata (Karoo Supergroup) dominated by shale, siltstone, and sandstone [Broquet, 1992; Cole, 1992; Cloetingh et al., 1992; Catuneanu et al., 1998]. Cole and Cloetingh et al. report a thickness of about 4600 m near the northern end of our profile. The Karoo Supergroup is subdivided from the top downward into the Beaufort, Ecca, and Dwyka groups. An important marker horizon in the Karoo Basin is a series of deep water carbonaceous shales within the Ecca Group (~40 m thick Whitehill and ~180 m thick Prince Albert Formations). In the southern part of the basin along the geophysical profile, the Karoo strata are tightly folded with north-vergence whereas deformation intensity decreases northward and strata have gentler dips.

[5] To the south the Karoo Basin is terminated by the Cape Fold Belt (CFB, Figure 1). This belt comprises a thick sequence of Neoproterozoic to early Paleozoic metasedimentary rocks (Cape Supergroup), which were deposited in a marginal basin created by inversion of a Pan-African Mobile Belt [de Wit, 1992]. The stratigraphy of the Cape Supergroup consists of a lower series up to ~3 km of Neoproterozoic to Cambrian metasediments in local basal rift sequences (e.g., Kango Inlier [Barnett et al., 1997]), which are overlain by ~8 km Ordovician to Carboniferous clastic sediments and orthoquartzites [Hälbich, 1983, 1993; Tankard et al., 1982; Broquet, 1992; Catuneanu et al., 1998]. Together with the lower units of the Karoo Basin (see above), the Cape Supergroup rocks were deformed at ~250 Ma, with the formation of north-vergent asymmetric or overturned folds and thrust faults [Hälbich, 1993; Hälbich and Swart, 1983]. The dominant CFB thrusts are

south dipping and may coalesce into a common decollement [Hälbich, 1983, 1993; Newton, 1992; Paton *et al.*, 2006]. Drill cores discussed by Eglington and Armstrong [2003] show that some of the Cape Supergroup underlies the Karoo Basin, but it is not known how far north the Cape Supergroup extends.

[6] The Cape Supergroup, and farther north the KB, unconformably overlie the Namaqua-Natal Mobile Belt (NNMB, Figure 1). This Mesoproterozoic complex has accreted to the lithospheric core of the Kaapvaal Craton, and experienced successive periods of extension and compression between 2.0 and 1.0 Ga [de Wit, 1992]. During the Late Proterozoic/Early Cambrian, eroded material from uplifts in the NNMB filled basins to the south, forming the Kango and Kaaimans Inliers [Hälbich, 1993]. The NNMB is a highly complex polymetamorphic province that constitutes three sub-provinces or terranes, which were amalgamated and attached to the Archaean Kaapvaal Craton during the late Mesoproterozoic [Robb *et al.*, 1999; Eglington and Armstrong, 2003; Raith *et al.*, 2003; Dewey *et al.*, 2006; Eglington, 2006, and references therein]. The age of peak metamorphism across all terranes was 1.02–1.04 Ga [Eglington, 2006], and assemblages indicate upper amphibolite to granulite-facies conditions with locally extensive generation of crustal melts now represented by megacrystic orthogneisses. The structural history of the NNMB includes regional ductile deformation with refolded recumbent folds, thrusting and listric shear zones that produced strong shallow to steeply-dipping fabrics and regionally extensional shear zones. Interpretation of a seismic refraction profile across the NNMB in the western Cape Province indicated crustal thickness of about 42 km and intermediate P-wave velocity of 6.2–6.9 km/s in the lower crust [Green and Durrheim, 1990]. Similar results were reported by Hirsch *et al.* [2008] from a combined interpretation and modelling of gravity and seismic data along an offshore-onshore profile which crosses the Orange Basin off the western coast of Southern Africa, and extends 100 km inland. The crustal thickness and lower-crustal P-wave velocity values at the inland end of this profile are 36–38 km and 6.7 to 7.0 km/s, respectively. The eastern exposures of the NNMB in KwaZulu-Natal comprise a number of litho-tectonic terranes dominated by upper amphibolite to granulite-facies gneisses with occasional charnockites, separated by subvertical ductile shear zones [Jacobs *et al.*, 1993; Jacobs and Thomas, 1994; Eglington, 2006; McCourt *et al.*, 2006].

[7] The profile crosses two major continental geophysical anomalies: the Beattie magnetic anomaly (BMA), and the Southern Cape Conductive Belt (SCCB). Both features stretch for more than 1000 km in a roughly east-west orientation (Figure 1). The BMA, a positive anomaly, was first observed by Beattie [1909]. Following a magnetometer array study, Gough *et al.* [1973] concluded that a large body with high electrical conductivity underlies the NNMB and parts of the KB. Gough interpreted this Southern Cape Conductive Belt as the signature of a linear plume in the upper mantle. However, de Beer *et al.* [1974] suggested that, due to their spatial coincidence, the two geophysical anomalies are likely to have a common source, and that such a plume could not account for the BMA. de Beer and Gough [1980] then used Curie isotherms to show that if a

common source exists, it must be a crustal feature. Pitts *et al.* [1992] suggested a sliver of serpentinized oceanic crust, 30 km broad and dipping south from a depth of 7 to 30 km as the source. However, a recent magnetotelluric study by Weckmann *et al.* [2007a] found no evidence for the existence of such an extensive high-conductivity body, which could be the source of the magnetic anomaly at the same time.

[8] The offshore section of this western profile starts about 20 km off the coast and stretches over 400 km south, past the Agulhas-Falkland Fracture Zone (AFFZ, Figure 1). Between the AFFZ and the present coast a network of basins, collectively referred to as the Outeniqua Basin (Figure 1), is located [e.g., Fouche *et al.*, 1992; McMillan *et al.*, 1997; Broad *et al.*, 2006]. This complex basin developed because of extensional episodes in Oxfordian/Kimmeridgian and Valangian times exploiting the structural gain of the underlying Cape Fold Belt [e.g., McMillan *et al.*, 1997]. The Outeniqua Basin is bounded to the south by a marginal ridge, which was first described by Scrutton and du Plessis [1973] and renamed into Diaz Marginal Ridge (DMR) by Ben-Avraham *et al.* [1997]. While earlier studies [e.g., Scrutton and du Plessis, 1973] describe it as a basement ridge, more recent studies by Parsieglia *et al.* [2007] suggest a metasedimentary composition of this ridge. South of the DMR, the AFFZ, a large-scale fracture zone, is located. The magnetic signature of this fracture zone was first identified by Ogoti [1964] south of Africa. The AFFZ marks the southern boundary of the African continent [Talwani and Eldholm, 1973]. This sheared continental margin developed as a consequence of dextral strike-slip motion between today's African and South American continents during the Cretaceous break-up of Gondwana [e.g., Barker, 1979; Rabinowitz and LaBrecque, 1979]. During this shear process the originally juxtaposed Southern Outeniqua and Falkland Plateau Basins were separated [e.g., Martin *et al.*, 1981; Ben-Avraham *et al.*, 1997] and the major faults of the Outeniqua Basin were bent [e.g., Ben-Avraham *et al.*, 1993; Thomson, 1999; Parsieglia *et al.*, 2007].

3. Seismic Data Acquisition

[9] The wide angle seismic experiment was carried out in April–May 2005. The 240 km onshore part [Stankiewicz *et al.*, 2007] consisted of 13 shots (each 75–125 kg of explosives) fired from boreholes 20–30 m deep (Figure 1). Forty-eight stations (average spacing of ~5 km) each consisting of a GPS synchronized electronic data logger (EDL) and a three-component seismic sensor were used to record the data. The offshore part (AWI-20050100 [Parsieglia *et al.*, 2007]) consisted of 20 four-component (three component seismometer and a hydrophone component) ocean bottom seismometers (OBS) deployed over 400 km profile length. Eight G-guns and one Bolt-airgun (volume of 96 l) were fired every 60 seconds during cruise SO-182 of the RV *Sonne*. This gave a shot spacing of approximately 150 m. As the onshore and offshore parts were carried out simultaneously, the airgun shots were recorded by the land receivers, improving the profile's ray

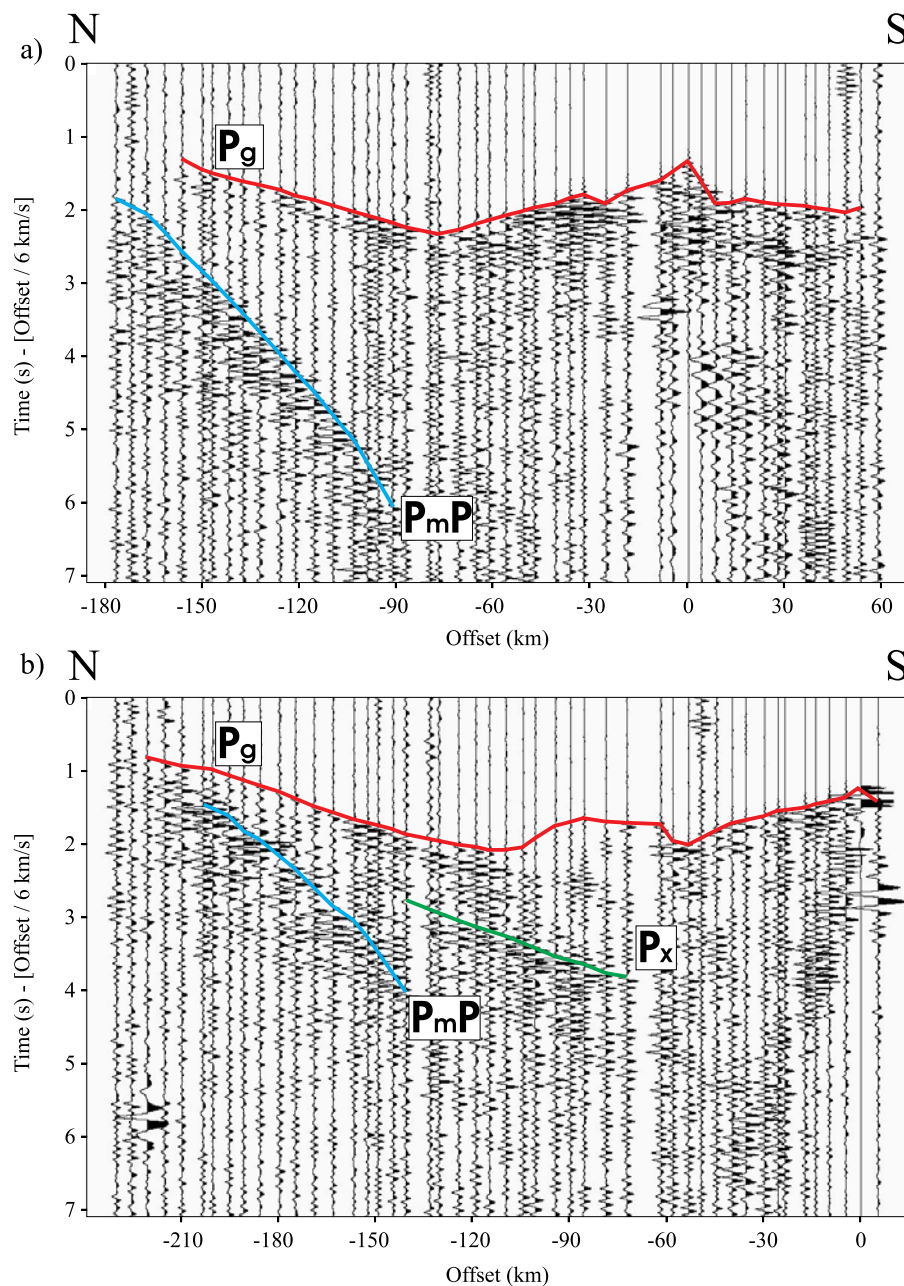


Figure 2. Examples of data recorded by land receivers from land shots. (top) Shot X10. The refracted P waves (P_g) are marked in red, and Moho reflections (P_mP) are in blue. (bottom) Shot X13. Phases reflected off the “floating” crustal reflector (P_x) are marked in green. Reduced traveltimes are shown with a reduction velocity of 6 km/s.

coverage, especially beneath the coast. Land shots were not detected by OBSs.

4. Wide-Angle Seismic Data Processing

[10] Figure 2 shows the high quality of the traces resulting from land shots, recorded by the land receivers. The direct (refracted) P-wave arrival (P_g , red), as well the Moho reflection (P_mP , blue) are clearly seen. Examples of airgun shots picked up by land receivers are illustrated in Figure 3, where, due to the longer offsets, the P waves refracted in the upper mantle (P_n) are also seen. The airguns produce much

less energy than the land shots, but because of their small spacing prominent arrivals can be easily identified. Examples of airgun signals registered by the OBS can be seen in Figure 4. All together, 24045 arrivals were manually picked (Table 1). Pick uncertainty was in the range of 0.05–0.25 seconds, depending on the signal to noise ratio.

[11] Two travel-time inversion techniques have been used in this study. Standard 2-dimensional tomography involves dividing the cross section beneath the profile into rectangular cells. An initial velocity model needs to be provided, and its values temporarily assigned to the cells. A simple one-dimensional model was used here. Synthetic traveltimes are

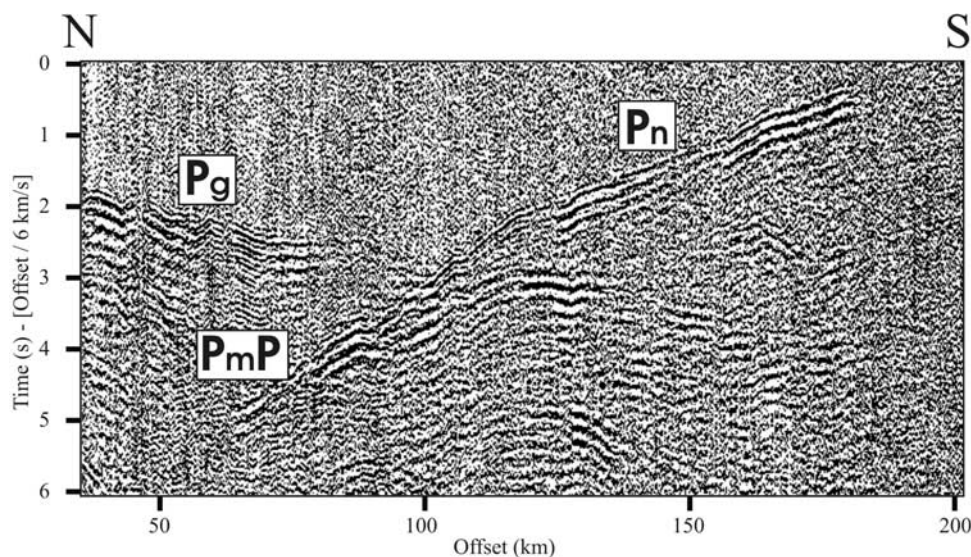


Figure 3. Example of the data from airgun shots picked up by land receiver 46. Direct P waves from the crust (P_g), from the mantle (P_n), and Moho reflections (P_mP) are clearly visible. Reduced traveltimes are shown with a reduction velocity of 6 km/s.

then computed, and compared to real (picked) ones. An iterative algorithm adjusts the individual values until an optimal model is reached. This study uses the software package FAST (First Arrival Seismic Tomography), which was released by *Zelt and Barton* [1998]. This package is a modification of the algorithm developed by *Vidale* [1988] to ensure a better detectability of high-velocity contrasts. To minimize the influence of the starting model, we have used an iterative approach developed by *Ryberg et al.* [2007], which repeats the inversion 5 times, using increasingly smaller cell sizes. We have performed the inversion using vastly different starting models, and found no significant differences in the resulting models. A ratio of 1:8 was used for the vertical-to-horizontal smoothing constraints.

[12] The above technique was used to compute the velocity model for the upper crust beneath the land section of the profile, as well as the northernmost 100 km of the offshore section. The final cell size used was 2 km hori-

zontal by 1 km vertical. For first-arrival tomography calculations it is important to have individual rays crossing each other in every individual cell, so having airgun shots spaced in only one direction from the receivers is not an optimal situation. For this reason only a small part of the offshore section was used, with the purpose of improving the onshore ray coverage rather than trying to compute a detailed offshore model. The resolving capabilities of the algorithm can be tested with checkerboard tests, where checkerboard of alternate positive and negative velocity anomalies is added to the originally computed velocity model. Synthetic traveltimes are then generated, and an inversion is performed using these times. The inversion result is then subtracted from the initial model. If the blocks can be observed in the final model, we can assume that a real feature corresponding to the block's size, position and velocity perturbation would be resolved by our inversion

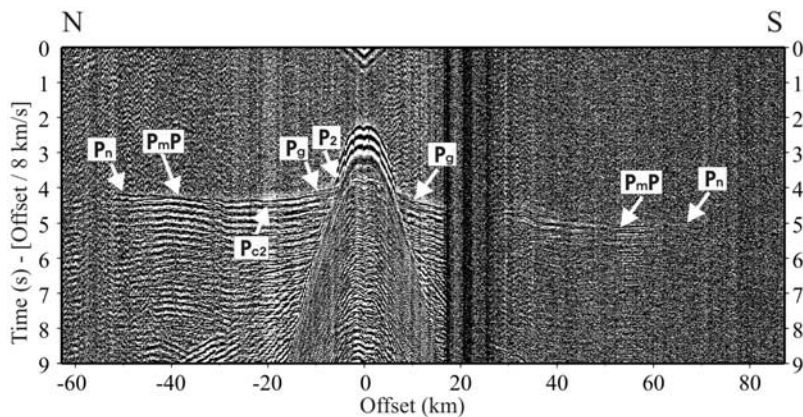


Figure 4. Airgun shots recorded by OBS 105. Phases P_g , P_n , and P_mP are as in Figure 3. P_2 corresponds to P waves refracted in the upper crust low-velocity sediments, and P_{c2} P waves are reflected inside the crust (notation from *Parsieglia et al.* [2007]). Reduced traveltimes are shown with a reduction velocity of 8 km/s.

Table 1. Number of Picked Arrival Times

Phase	Airgun, OBS	Airgun, EDL	Land Shot, EDL	Σ
Crustal refraction	2329	5030	445	7804
Mantle refraction	225	13,861	0	14,086
Moho reflection	642	1028	132	1802
Intracrustal reflection	332	0	21	353
Σ	3528	19,919	598	24,045

algorithm, and therefore an observed feature like that is likely to be real, and not an inversion artifact.

[13] A disadvantage of FAST is that reflected phases cannot be incorporated in the model. For this reason, the travel-time routine RAYINVR [Zelt and Smith, 1992] was used. In this program the 2-D velocity model is defined in terms of layers. Velocity is specified at a number of nodes along the layer boundaries, and a linear velocity gradient is assumed between nodes (both along boundaries, and with depth). Rays may refract in a particular layer, reflect off any boundary, or travel as head waves along it. As with FAST, model quality is determined by comparing synthetic traveltimes to the manually picked real ones. Modelling is done as an iterative combination of forward modelling and inversion [Zelt and Forsyth, 1994]. The resolution of the velocity model depends (among other things) on the number of layers defined, and the node density along them. The marine model of Parsieglia *et al.* [2007] was computed using this package. Their model consists of 6 layers: a water layer, two sedimentary layers, two crustal layers and the mantle.

[14] To produce a starting velocity model for the joint onshore-offshore analysis of the entire profile, the two separate models had to be merged. As a number of reflected phases are available, RAYINVR was considered the more appropriate package to use. For this reason, the onshore FAST model needed to be converted into a layered model, with layers matching the ones in the offshore model. The uppermost sedimentary layer (marine sediments), and obviously the water layer, exist only in the offshore section, so the onshore part consisted of 4 layers. The uppermost of these was a shallow (not exceeding 3 km) zone with velocities typical for sedimentary rocks. The next 2 layers represented the crystalline crust. In the starting model they were separated at a depth of 15 km, using velocities obtained from the FAST at nodes spaced 20 km apart. The boundary between the 3rd and 4th layer was the Moho, set in the starting model at 42 km [after Lindeque *et al.*, 2007]. The combined starting velocity model is then iteratively updated, using forward and inverse modelling, until the calculated synthetic traveltimes match the data as well as possible. While converting from FAST to RAYINVR decreased the resolution of small-scale features in the onshore part, the two modelling techniques complement each other, and our final results are better than what could be achieved using either of the techniques alone.

5. Results

5.1. Crustal Features Beneath the Continent

[15] The upper crust model computed with FAST using first arrivals of land shots (445 P-wave arrivals), as well as

airgun shots less than 100 km from coast (3351 P-wave arrivals), is shown in Figure 5. The RMS traveltimes residual was 0.045 seconds, and the chi-squared misfit parameter 2.60. Figure 5 needs to be viewed in conjunction with Figure 6, which shows the checkerboard tests conducted on the model. These tests confirm that the model is better resolved beneath the land, where features barely twice as wide as the receiver spacing can be resolved in the upper 10 or 15 km. Large-scale features, 40 km wide, can be confidently resolved almost to the maximum ray penetration, even beneath the ocean.

[16] The model in Figure 5 is consistent with the model computed using only onshore shots [Stankiewicz *et al.*, 2007]. However, the improved ray coverage increased the maximum depth of the model from less than 30 km to almost 40 km, and many of the upper crustal features are better resolved. In the northern half of the profile, the slow velocities (4.6–5.3 km/s, red and orange in Figure 5) characterizing the Karoo Basin are clearly visible to depths not exceeding 5 km. Slightly faster (5.4–5.8 km/s, yellow and pale green) velocities beneath indicate the relatively thin Cape Supergroup. The resolution of the model does not clearly indicate the contact of the two supergroups. The checkerboard tests indicate that the thinning of the basin at profile length of 100 km is a real feature – this is consistent with our earlier results [Stankiewicz *et al.*, 2007], which suggested a blind Paleozoic Thrust Fault, which could mark the northernmost deformation of the Cape Supergroup. The thickening of the basin at profile length of approximately 130 km (also well within the resolving capability of the model) is consistent with the large asymmetric syncline inferred from field observations [Cole, 1992].

[17] Farther south, the geometry of the listic Kango Fault (KF) is resolved much more clearly than in the earlier results [Stankiewicz *et al.*, 2007]. Near the surface (at ~ 170 km profile length) this fault marks the northern edge of the Jurassic Uitenhage basin, characterised by very low velocities (~ 4.5 km/s). The offshore section of the model is not well resolved, which was expected from the shot-receiver geometry explained in the previous section. However, the very low velocities representing the sediment cover (< 5 km/s) are clearly seen to be significantly deeper than onshore.

5.2. Combined Onshore-Offshore Model

[18] The final RAYINVR model is shown in Figure 7. The programme used 21,868 traveltimes (over 90% of the picks). The RMS traveltimes residual was 0.134 seconds, which is within the uncertainty bounds of individual picks. The chi-squared misfit parameter was 1.74. Table 2 shows how these uncertainties vary for different phases. A value greater than 1 for the chi-squared parameter means the small-scale features of the model have not been resolved [Zelt and Forsyth, 1994], so we will concentrate our discussion on the large-scale features. A likely explanation for a large value of chi-squared is the presence of 3-D effects, in particular the fact that the onshore and offshore parts of the profile are not perfectly aligned (Figure 1). Examples of ray paths in the model are shown in Figure 8. The relative ray coverage available is shown in Figure 9, with red areas indicating poor ray coverage.

[19] In addition to the standard phases P_g and P_mP , an unusual phase has been observed on the traces recorded

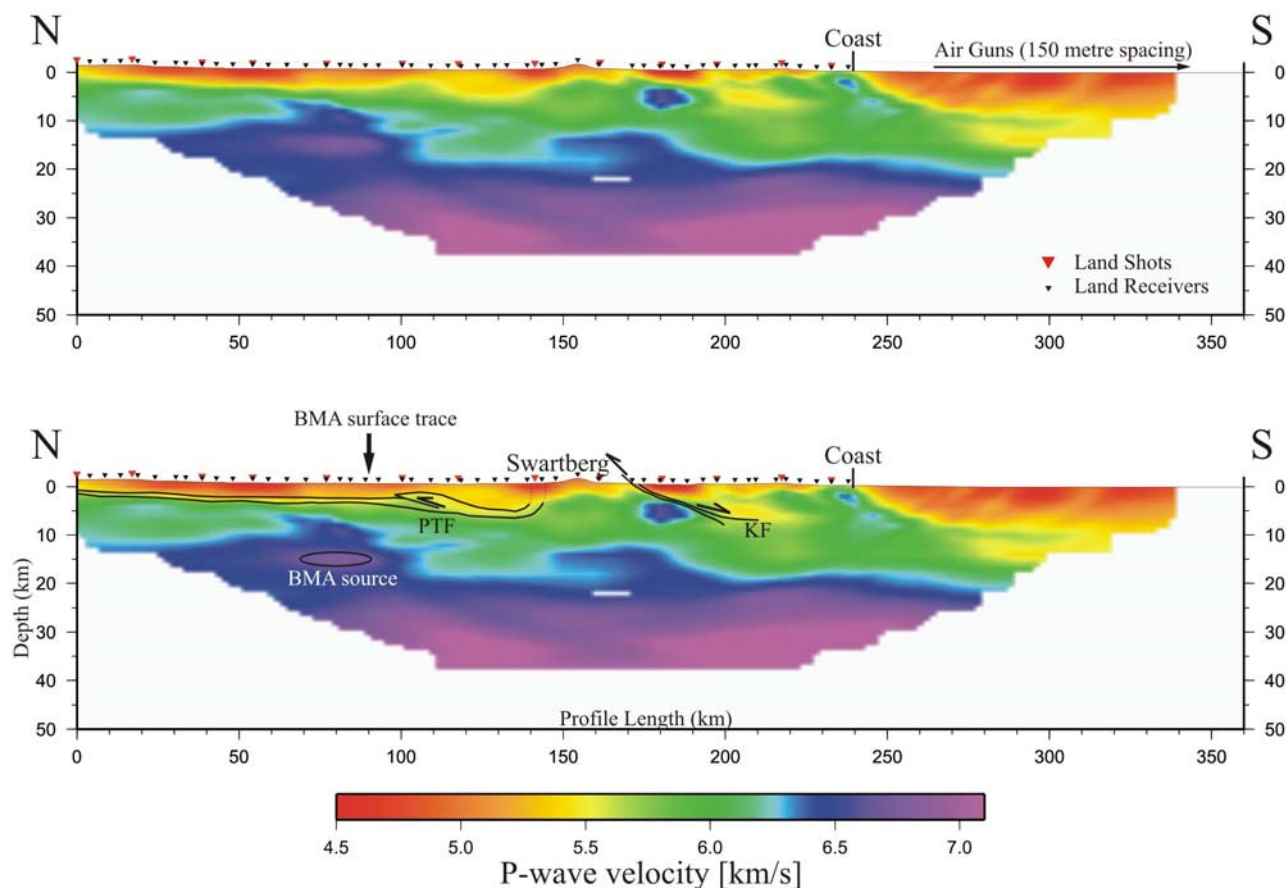


Figure 5. P-wave velocity model computed for the onshore part of the profile, as well as the first 100 km of the offshore part. The top shows just the model, the bottom includes interpretations. Starting in the north, 140 km of the inferred distribution of the Karoo Supergroup, and the Cape Supergroup underlying it, has been drawn. The location of the blind thrust fault, which we believe marks the northernmost deformation of the Cape Supergroup, has been marked by an arrow (PTF). We see the thickening of the basement at profile km 130, which is consistent with the syncline at which it tapers out. The actual edge of it, however, is not resolved and has been drawn in dotted lines. Farther south, the geometry of the normal listric Kango Fault (KF, surfacing at 170 km) has been drawn. A high-velocity anomaly most likely related to the BMA has been indicated with an ellipse at a depth of ~ 15 km, at profile km 80. The center of the surface trace of the BMA has also been indicated.

from the two southernmost shots (P_x , Figure 2). The amplitude of this phase is of similar order of magnitude to the P_mP . Furthermore, the phase is most prominent in the vertical component, so we interpret it as P waves reflected inside the crust. As a reflected phase, these traveltimes could not be included in the FAST model, and the corresponding reflector location was derived with RAYINVNR using the floating reflector technique. The position of the reflector that best fits the observed traveltimes was found to be between profile km 190 and 220, rising steeply southward from a depth of 35 km to 23 km (Figure 7). The steep landward dip of this reflector makes it impossible to detect reflections of airgun shots off it, the same way the steeply rising Moho was invisible.

[20] The most interesting feature of the joint model shown in Figure 7 is the Moho discontinuity, clearly visible as a high-velocity contrast. The Moho depth beneath the Karoo Basin is ~ 40 km, and slightly deeper (~ 42 km) beneath the CFB. The crustal thickening beneath the CFB is consistent with receiver function analyses [Harvey et al.,

2001; Nguuri et al., 2001]. However, the study by Nguuri et al., while detecting the thickening, consistently locates the Moho approximately 5 km deeper than reported here. This could be due to the fact that these authors use an average crustal velocity of 6.5 km/s. This value is typical for the Kaapvaal Craton at which their study was aimed, but is too high for off craton analysis. Our results are much closer to those of Harvey et al., who subdivided the crust into regions of different velocity at different depths.

[21] South of the CFB the Moho depth becomes shallower very abruptly, reaching 30 km at the present coast. The depth is consistent with values obtained from an east-west reflection profile of Durrheim [1987], which runs approximately 10 km south of the coast. Farther south the crust continues to thin, albeit much more gradually, for another 250 km, underneath the Agulhas Bank, Outeniqua Basin and the Diaz Marginal Ridge, until it reached the Agulhas-Falkland Fracture Zone (AFFZ). This fracture zone marks the continent-ocean transition (COT). This transition to oceanic crust begins around profile distance of 480 km,

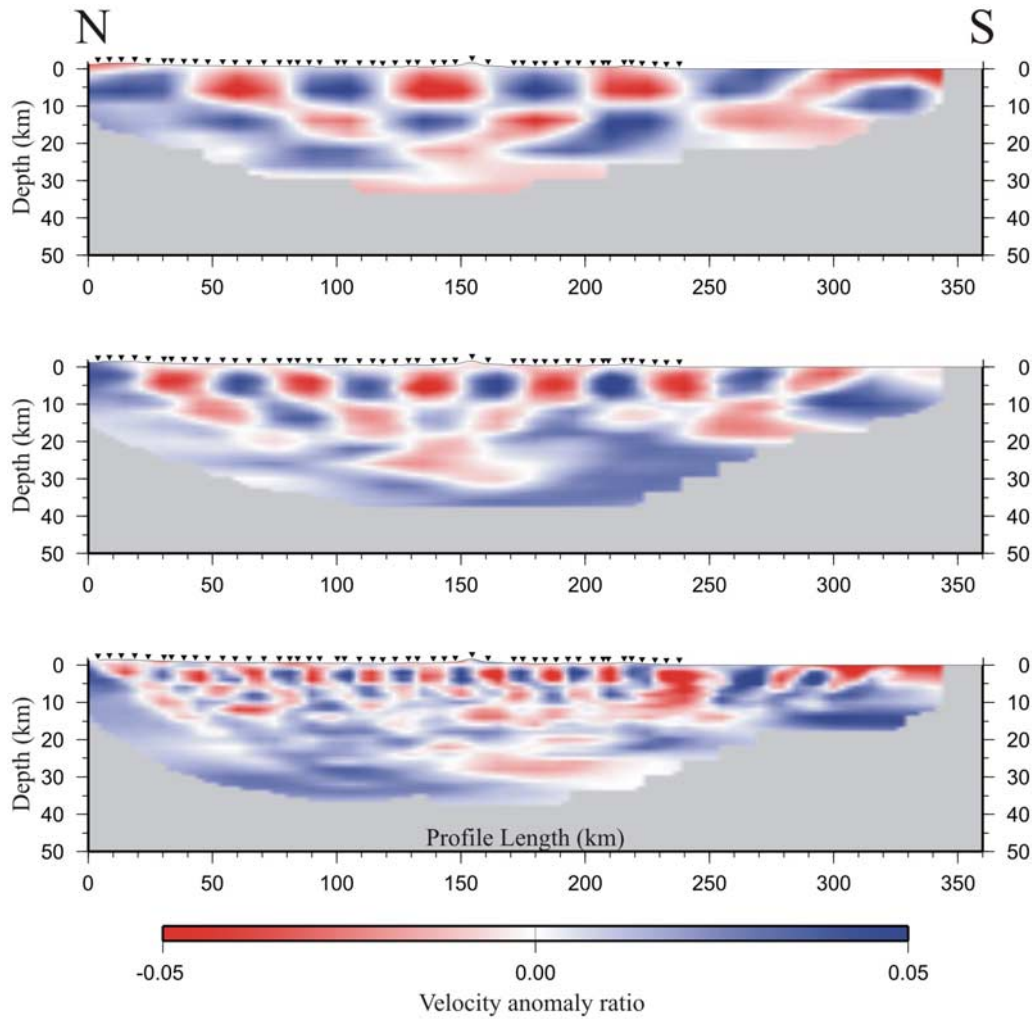


Figure 6. Resolution tests for the model in Figure 5. Original checkerboard sizes are (top) 40 × 10 km, (middle) 25 × 10 km, and (bottom) 12 × 5 km; velocity perturbation of 5% is used in each case.

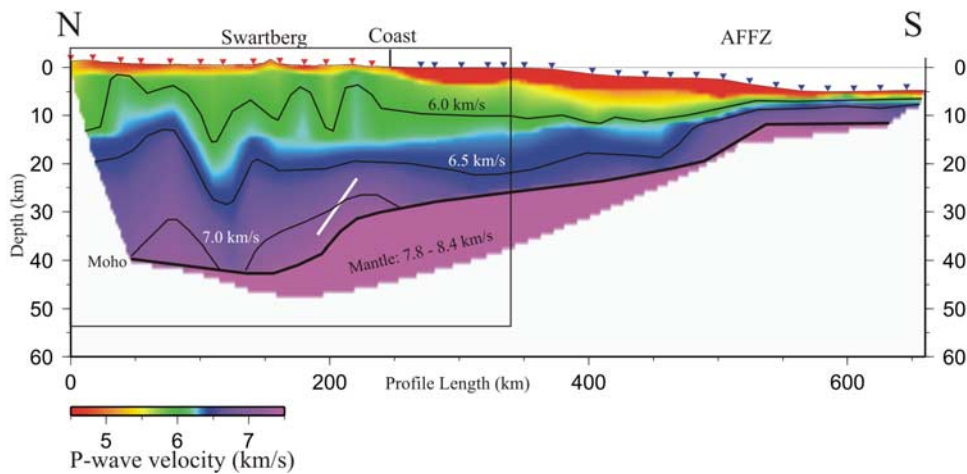


Figure 7. P-wave velocity model for the entire profile. To help the location with Figure 1, land shots (red triangles) and OBSs (blue triangles) have been indicated. Velocity contours corresponding to 6.0, 6.5, and 7.0 km/s have been drawn. The thick white line marks the “floating” reflector. The black rectangle indicates the northern 340 km that is shown in Figures 5 and 6.

Table 2. Model Quality for Different Phases

Phase	RMS	χ^2
Crustal refraction	0.132	1.70
Mantle refraction	0.132	1.70
Moho reflection	0.161	2.40
Intracrustal reflection	0.173	0.88
Σ	0.134	1.74

where the Moho depth of 20 km is reduced to 12 km over a little over 50 km horizontal difference [Parsieglä *et al.*, 2007]. This is a typical length, as well as depth change, for the transition at sheared margins [e.g., White *et al.*, 1992; Bird, 2001]. The depth of 11–12 km (i.e., 6–7 km of crust under 5 km of ocean) is observed in the Agulhas Passage, where the southernmost 130 km of the profile stretches.

6. Discussion

6.1. Crustal Features Beneath the Continent

[22] Most of our shallow results are consistent with the results of the magnetotelluric profile [Weckmann *et al.*,

2007a] coinciding with the northern 140 km of the seismic line. These authors traced the highly conductive Whitehill Formation (pyrite-rich black shales at the bottom of the Ecca Group) for virtually the entire length of their profile, which correlates well with the geometry of the basin obtained with our tomography. The accuracy of the Whitehill's location in the MT depth section is confirmed by excellent correlation with drill cores [Eglington and Armstrong, 2003; Branch *et al.*, 2007]. Weckmann *et al.* also observe an offset in the depth to the shales at the same location as our basement thinning, and also suggest a south dipping thrust as a likely explanation.

[23] There is also some correlation between the velocity model and the electrical conductivity image of Weckmann *et al.* [2007a] for deeper features (Figure 10). Our model shows a zone of anomalously high velocity (~ 7 km/s) at a depth of ~ 15 km between profile km 60 and 90. The size of the body certainly falls within the model's resolving capability. The southern edge of this anomaly is in the vicinity of the center of the BMA. In the 2D image of the electrical conductivity distribution, a zone of high electrical resistivity is found at the same location. To the north this

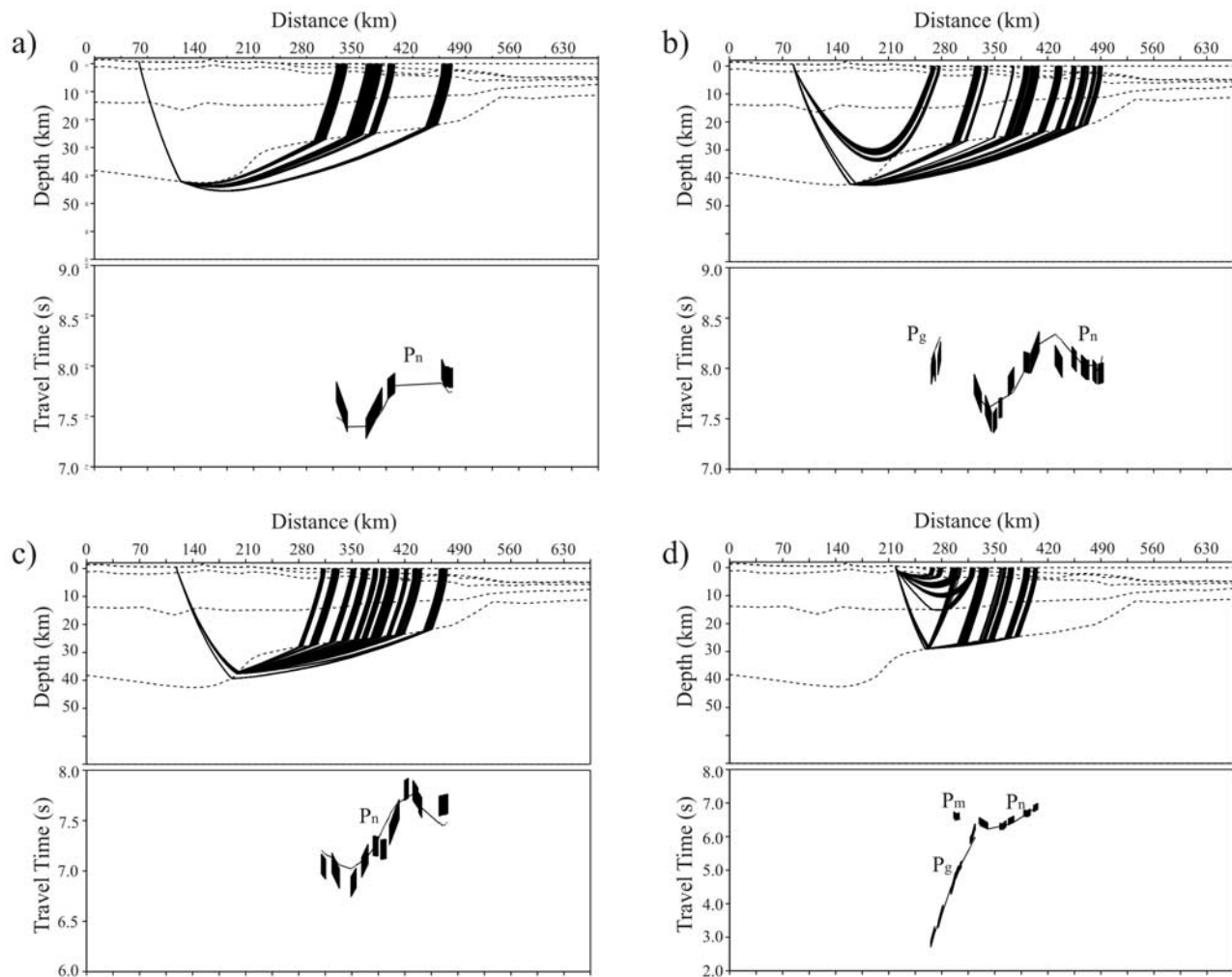


Figure 8. Airgun shots recorded by 4 land receivers: (a) receiver 12; (b) 17; (c) 24; (d) 44. (top) The raypaths; (bottom) the observed traveltime (steeples corresponding to uncertainty bars) and the traveltime expected from the model for the given source-receiver distance (solid line).

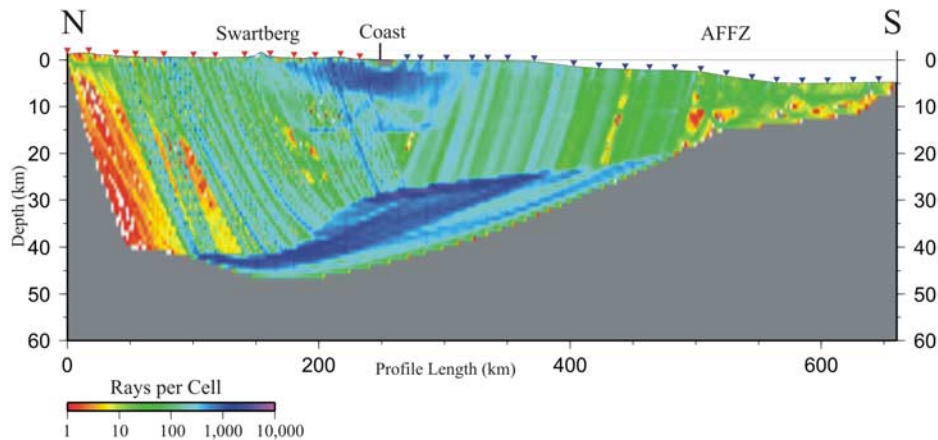


Figure 9. Ray coverage for the model presented in Figure 7. A logarithmic scale of number of rays crossing each 2 km by 1 km cell highlights regions of relatively high or low coverage.

zone is flanked by a large mid-crustal region of stacked layers of high electrical conductivity, possibly imaging mineralizations in synforms, and, to the south, by a narrow, southward dipping conductor at 7–15 km depth under the maximum of the BMA. The top of this anomaly is exactly coincident with what a seismic reflection study [Lindeque *et al.*, 2007] called a “complex seismic reflectivity patch”. However, a comparison of magnetic models explaining the magnetic response of the BMA with the electrical conductivity model clearly shows that the electrical conductivity anomaly located beneath the center of the BMA is too narrow to be a possible source of the BMA [Weckmann *et al.*, 2007b]. Figure 10 shows the two magnetic bodies outlined by black lines, each with a magnetic susceptibility of 0.05 SI. Weckmann *et al.* show that these simple magnetic bodies would produce a response similar to the signature of the BMA. The bodies are separated by a fault, which cuts through at the same inclination as the conductivity anomaly. The gap (some 100 m wide) representing the fault has an induced magnetic susceptibility of 0.0 SI, the same value as the background susceptibility. The location of the fault correlates well (at least in the upper 20 km) with the velocity contrast marking the northern edge of the synclinal low-velocity zone between 100 and 140 km along the profile, while the top of the northern body correlates very well with both the high-velocity anomaly and the zone of high resistivity north of the surface maximum of the BMA [Weckmann *et al.*, 2007a; Y. Quesnel *et al.*, Local modelling of the Beattie magnetic anomaly in South Africa, manuscript in preparation, 2008].

6.2. Combined Onshore-Offshore Model

[24] The geometry and seismic velocity structure derived from a joint interpretation of onshore and offshore V_p tomography (Figure 7) provides one of the best available geophysical images of a sheared continental margin in cross-section. It also allows a detailed comparison with features from profiles across the classic volcanic rifted margins on the western coast of South Africa. The most direct comparison is with the seismic profile across the Orange Basin [Hirsch *et al.*, 2008], because this profile also extends oceanward from the Namaqua-Natal Mobile Belt. The sheared and volcanic margin profiles are compared at

the same scale on Figure 11. Both profiles show similar wedge-shaped geometry and furthermore, the crustal thickness (Moho depth) does not reduce uniformly but stepwise, with inflection points separating segments of rapid and gradual change. Comparing these segments in turn, from the continental crust (A in Figure 11) outward, we consider the following observations most important:

[25] 1. Both profiles begin at the landward end in the Namaqua-Natal Mobile Belt, in the case of the Karoo-Agulhas profile this is covered by the Karoo sequence. The crustal thickness at this end of both profiles is about 40 km, but there is a major difference in the seismic velocity structures of the lower crust. The Karoo-Agulhas profile shows a zone up to 7 km thick with seismic velocity above 7.0 km/s (maximum $V_p = 7.4$ km/s), whereas the basal velocity at the Springbok profile does not exceed 6.8 km/s. The significance of the high-velocity lower crust is discussed in more detail below. The high-velocity zone on the Karoo-Agulhas profile is interrupted at profile distance 120 km by a “keel” of material with intermediate velocity (green on Figures 7 and 11). The higher resolution of the upper crustal seismic image (Figure 5) shows that this feature has a complex shape that appears consistent with the north-vergent folds and thrust faults known in the upper crust.

[26] 2. Over much of the segment of stretched continental crust (B in Figure 11) between continental crust (segment A) and the steep decrease in Moho depth (segment C), the crustal thickness at the Karoo-Agulhas profile is significantly greater at the Springbok profile. This is likely due to the presence of the Cape Fold Belt, which is not intersected by the Springbok profile on the west coast.

[27] 3. The stretched crust shows a gradual and uniform thinning on the sheared Agulhas margin. The lower crustal seismic velocity in this segment is also uniform, with V_p values of 6.5 to 7.0 km/s that are in the same range as the lower crust observed in other parts of the NNMB [Green and Durrheim, 1990; Durrheim and Mooney, 1994; Hirsch *et al.*, 2008]. This is in marked contrast to the corresponding segment on the Springbok VRM, which shows a downwarping of the lower crust in the middle part of the segment. This “keel” has a higher seismic velocity ($V_p > 7.0$ km/s) than the lower crust elsewhere along the profile, and even

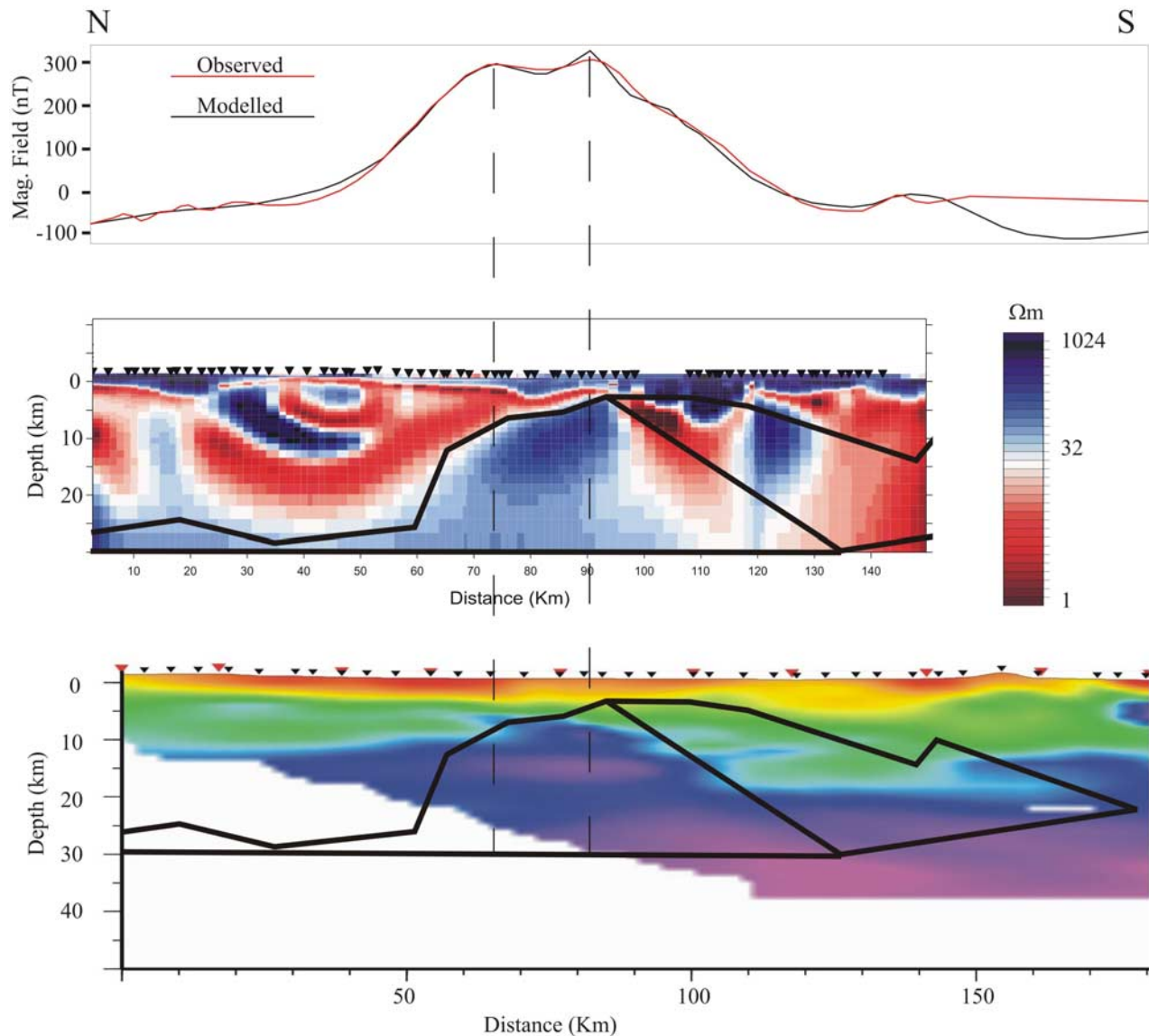


Figure 10. (top) Surface magnetic field (red line) along the profile, compared to the modeled magnetic signature of two magnetic bodies intersected by a few 100 m wide nonmagnetic region [Weckmann *et al.*, 2007b]. (middle) The two magnetic bodies drawn over the MT depth section of Weckmann *et al.* [2007a]. (bottom) The magnetic bodies drawn over the northern 180 km of the P-wave velocity model shown in Figure 5. Vertical dashed lines across all three figures project the locations of the maxima of the BMA onto the depth sections.

the crust above the keel has a higher velocity than at the same depth outside the keel region. High-velocity lower crust are very common features at volcanic rifted margins and interpreted as underplated basaltic magma that intruded and ponded at the crust-mantle boundary [Menzies *et al.*, 2002]. Hirsch *et al.* [2008] showed that this interpretation is consistent with gravity modelling of the Springbok profile and also noted that the high-velocity keel underlies a zone of seaward-dipping reflector wedges in the upper crust, also characteristic features of volcanic rifted margins and interpreted as submerged basalt flows on the foundering margin [Menzies *et al.*, 2002]. Note that if the high-velocity keel on the Springbok profile is considered to be accretion of new crust by magmatism, the geometry of the Springbok margin

in this segment is very similar to that of the Agulhas margin, with a uniform, moderate thinning (dashed line, Figure 11).

[28] 4. Both margins exhibit an abrupt rise of the Moho over about 50 km (segment C). In the case of the Agulhas margin, the lower crust at this rise shows a higher seismic velocity than in the “stretched” segment, with values of about 7 km/s. This represents the continent-ocean transition across the sheared margin. For the Springbok profile this increase in seismic velocity at the steep rise is not observed, because it is part of a much longer (~200 km) continent-ocean transition zone.

[29] 5. The oceanic crust (segment D) on both sections has the global average thickness of about 7 km and a velocity structure that is also typical of oceanic crust worldwide. The postrift sedimentary cover on the oceanic

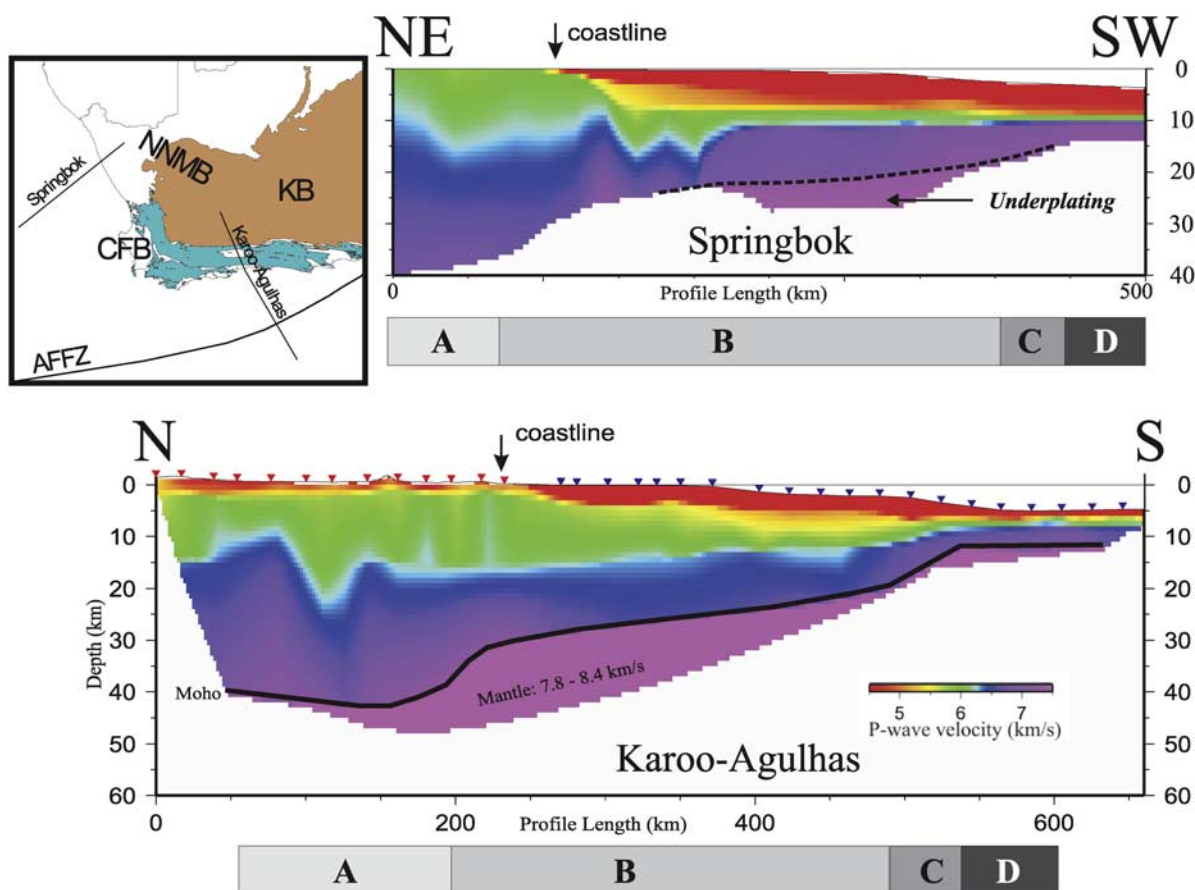


Figure 11. P-wave velocity model comparison between (top) the Springbok profile on the western coast of South Africa [after Hirsch *et al.* 2008] and (bottom) this study. On the basis of Moho geometry, four segments of the crust can be distinguished in both profiles: (A) thick continental, (B) stretched gradually thinning, (C) steeply thinning, and (D) thin oceanic crust.

crust at the Springbok profile is considerably thicker than at the Agulhas profile because it crosses the Orange River Basin.

[30] A number of theoretical and empirical models exist that link observed geometry and seismic properties with the processes of rifting and magmatism at volcanic rifted margins [e.g., Menzies *et al.*, 2002]. It is clear from their work that seaward-dipping reflector sequences in the upper crustal section land-ward of the ocean-continent transition zone, and thick, high-seismic-velocity lower crust (>7.0 km/s) underneath the reflector sequences result from massive intrusion of breakup-related magma. Classic examples of these features were documented from the Walvis Basin in Namibia by Bauer *et al.* [2000], and Trumbull *et al.* [2002] showed that the thickness (20 km) and high V_p -values (7.2–7.4 km/s) of underplated lower crust in NW Namibia require high mantle temperatures and active mantle upwelling, consistent with the proximity to the Walvis Ridge and Paraná-Etendeka Large Igneous Province. The volcanic rifted margin at the Orange River Basin (Springbok profile) is located some 1500 km south of the Walvis Ridge and the underplated crustal body is considerably thinner and has a lower average V_p velocity [Hirsch *et al.*, 2008]. Trumbull *et al.* [2007] found that dolerite dykes exposed along the coast from NW Namibia to the Cape Province showed a system-

atic decrease in their maximum MgO contents, both in whole-rock and in olivine, which is consistent with a waning plume influence from north to south expressed in lower mantle potential temperature and less active upwelling.

[31] On the sheared Agulhas margin, neither seaward-dipping reflectors nor high-velocity lower crust are revealed by the geophysical surveys, nor is there geologic evidence for synrift magmatism onshore. This margin can thus be considered as nonmagmatic with respect to the time of breakup. There is, however, seismic evidence of post-breakup magmatism on the profile. Seismic reflection sections in the Agulhas Passage found signs of volcanic seamounts and intrabasin reflectors interpreted as basaltic flows [Parsieglia *et al.*, 2007]. A late Cretaceous age of extensive volcanism (ca. 100 Ma) is also suggested from seismic data from the Agulhas Plateau [Uenzelmann-Neben *et al.*, 1999; Parsieglia *et al.*, 2008].

[32] One feature of the Karoo-Agulhas profile that deserves further comment is the zone of high seismic velocity ($V_p > 7.0$ km/s) in the lower crust inland of the coast (from profile km 150 to the coast). Whereas the velocity of this zone is like that encountered in underplated lower crust at volcanic rifted margins, the position of this zone in relation to the continental margin makes it unlikely

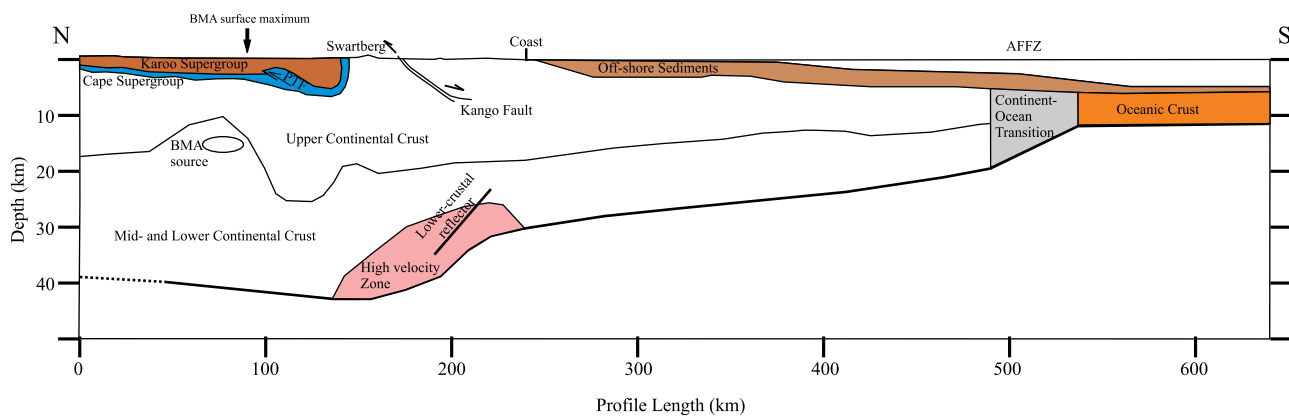


Figure 12. The combined onshore/offshore profile, showing the summary of the findings of this study. To the north the Karoo and Cape supergroups taper out in an asymmetric syncline. The division between upper and middle/lower crust roughly follows the P-wave velocity of 6.5 km/s contour. Near its most shallow point, the high-velocity anomaly most likely related to the BMA is found in the middle crust. Immediately south a large synclinal feature was identified in the upper crust. In the lower crust, high-velocity material has been observed on top of the steeply rising Moho, as was a reflector roughly parallel to the Moho. Offshore the layer of sediments can be seen, as is the structure of the AFFZ, which separates the continental from oceanic crust.

to represent breakup-related magmatism. Also, as mentioned above, there are no matching expressions of magmatism in the upper crustal seismic data, or on land. Crustal rocks with P-wave velocities greater than 7 km/s are most likely to represent mafic igneous rocks rich in olivine, or their metamorphosed equivalents (amphibolites, mafic granulites). Seismic velocities of metabasic rocks are particularly high if they are rich in garnet [e.g., *Durrheim and Mooney, 1994; Christensen and Mooney, 1995*]. *Gernigon et al. [2004]* discussed the likelihood of older high-pressure rocks (garnet granulite, eclogite) as an explanation for high Vp lower crust on parts of the rifted Vøring Basin in the Norwegian Sea. Considering the geologic setting of the Karoo-Agulhas profile, there are principally two possible explanations for the high-velocity crust. Either it represents metabasic lithologies of Precambrian age in the NNMB, or mafic intrusions added to the base of the crust by younger magmatism. The dominant exposed lithologies of the high-grade unit in the NNMB (Namaqualand terrain) are intermediate to felsic gneisses and meta-granitoids [*Dewey et al., 2006*]. These authors suggested that the heat source for granulite-grade metamorphism and crustal melting was “massive underplating” of mafic magmas at around 1050 Ma. The evidence cited for this underplating was a seismic refraction study by *Green and Durrheim [1990]*, who reported lower crustal velocities of 6.6–6.9 km/s for the western Namaqualand crust. Similar values of 6.8 km/s were derived for the base of the crust in the NNMB at the landward end of the Springbok profile [*Hirsch et al., 2008*]. Even under the thick Kaapvaal Craton, seismic data indicate a generally sharp transition from the Moho to crustal rocks with intermediate to felsic properties [*Durrheim and Mooney, 1994; Nair et al., 2006*] and no evidence for widespread high-Vp lower crust. Crustal xenoliths of garnet granulite are not uncommon in kimberlites from the NNMB [*Schmitz and Bowring, 2004*], and thus some high-Vp material must be present in the crust, however the seismic surveys so far undertaken

indicate that such material cannot be a major component of the lower crust. Therefore, although we do not rule out the possibility that the high-Vp zones at the base of the crust in the Karoo-Agulhas profile are part of the Proterozoic basement, all other studies of the NNMB and cratonic crust failed to detect velocities above 6.9 km/s.

[33] The alternative explanation for the high Vp values observed at the landward end of the Karoo-Agulhas profile is that Phanerozoic magmatism added thick intrusions of gabbroic material in the lower crust. This is of course the same scenario offered to explain the very common thick underplated crust at volcanic rifted margins, and it is clear from many studies that appropriate volumes of material and bulk seismic properties would fit the observations (7 km thickness, $V_p = 7.0\text{--}7.4$ km/s; see Figure 7). From the regional geology and location of the profile, the most likely candidate for producing extensive mafic underplating is the mid-Jurassic Karoo-Ferrar-Chon Aike Large Igneous Province. This was one of the major episodes of mafic magmatism on a global scale, and it is unlikely that the huge volumes of magma represented by Karoo lavas, dykes and sill complexes could be emplaced at upper crustal levels without an intrusive equivalent at depth. Unfortunately, the seismic experiments used in this study did not produce enough S-wave information to allow calculation of V_p/V_s ratios which would provide better lithologic discrimination, but from the available shape, location and Vp values of the lower crustal zone we believe an origin from underplated magmas related to the Karoo LIP provides the best explanation.

[34] *de Wit [2007]* already noted the surprising lack of seismic evidence for mafic underplating of the Karoo magmas, whereas such evidence is clear and abundant for the Paraná-Etendeka LIP on the western margin. We argue from the results of this study that significant Karoo underplating did occur. Its paucity in seismic studies under the craton probably relates to the deflecting action of the thick Kaapvaal lithosphere. Why there is no seismic expression

for underplating in the other surveys of the NNMB surveys is less clear but it may be related to the fact those surveys were located farther west than the Karoo-Agulhas profile whereas the locus of strongest Karoo magmatism is to the east, in the Lebombo-Natal and Lesotho regions.

7. Summary

[35] In this study we have used tomographic inversion of reflected and refracted traveltimes to construct a P-wave velocity model along an off-onshore profile across the southern margin of Africa. The findings are summarized in Figure 12. A number of the model's features agree with known geological record, and are consistent with the results of the separate onshore [Stankiewicz *et al.*, 2007] and offshore [Parsieglia *et al.*, 2007] analyses. These include the rough geometry of the Karoo and Cape supergroups, the presence of a blind Paleozoic Thrust Fault ~40 km north of the farthest Witteberg Group outcrop which possibly marks the northern edge of deformation in the Cape Supergroup, and the geometry of the Agulhas-Falkland Fracture Zone which marks the continent-ocean transition.

[36] New findings of this study are:

[37] 1. A high-velocity anomaly north of the center of the BMA is much better resolved than previously. This feature is coincident with an extensive zone of high resistivity and a magnetic body required to reproduce the magnetic signature of the BMA.

[38] 2. A synclinal low-velocity feature was identified in the Mesoproterozoic basement beneath the front of the Cape Fold Belt, south of the above mentioned feature. The northern edge of this feature correlates with the second magnetic body necessary to account for the BMA's signature.

[39] 3. A steep decrease in crustal thickness (from 40 to 30 km over lateral distance of 40 km) occurs under the present coast.

[40] 4. A zone of high-velocity material is observed in the lower-most crust beneath the present coast. This either represents metabasic lithologies of the Mesoproterozoic Namaqua-Natal Metamorphic Complex, or intrusions of gabbroic material added to the base of the crust by younger magmatism.

[41] **Acknowledgments.** J.S. thanks the GeoForschungsZentrum Potsdam for providing a scholarship to conduct research in Potsdam as part of the capacity building program of the Inkaba yeAfrica project. Equipment for the onshore experiments was provided by the Geophysical Instrument Pool, Potsdam. We thank the seismic and MT field teams, as well as the farmers who granted us access to their land. Many thanks go to the captain, the crew, and the scientific participants of the RV *Sonne* cruise SO-182. We are grateful to Ernst Flüh of IFM-GEOMAR for lending us OBS systems. The SO-182 cruise (project AISTEK-I) and N.P.'s position was funded by the German Bundesministerium für Bildung und Forschung (BMBF) under contract 03G0182A. The German Academic Exchange Service (DAAD) funded a 1 month research visit of N.P. to the University of Cape Town (South Africa). We thank Maarten de Wit for his continuous involvement in the project, as well as Klaus Bauer and Oliver Ritter for many discussions. The manuscript benefited from constructive reviews by Ray Durrheim and an anonymous reviewer. This is Inkaba yeAfrica publication 29.

References

- Barker, P. F. (1979), The history of ridge-crest offset at the Falkland-Agulhas Fracture Zone from a small-circle geophysical profile, *Geophys. J. R. Astron. Soc.*, *59*, 131–145.
- Barnett, W., R. Armstrong, and M. J. de Wit (1997), Stratigraphy of the upper Neoproterozoic Kango and lower Paleozoic Table Mountain groups of the Cape Fold Belt revisited, *S. Afr. J. Geol.*, *100*, 237–250.
- Bauer, K., S. Neben, B. Schreckenberger, R. Emmermann, K. Hinz, N. Fechner, K. Gohl, A. Schulze, R. B. Trumbull, and K. Weber (2000), Deep structure of the Namibia continental margin as derived from integrated geophysical studies, *J. Geophys. Res.*, *105*(B11), 25,829–25,853.
- Beattie, J. C. (1909), *Report of a Magnetic Survey of South Africa*, Royal Society of London Publication, Cambridge Univ. Press, London.
- Ben-Avraham, Z., C. J. H. Hartnady, and J. A. Malan (1993), Early tectonic extension between the Agulhas Bank and the Falkland Plateau due to the rotation of the Lafonia microplate, *Earth Planet. Sci. Lett.*, *117*, 43–58.
- Ben-Avraham, Z., C. J. H. Hartnady, and K. A. Kitchin (1997), Structure and tectonics of the Agulhas-Falkland Fracture Zone, *Tectonophysics*, *282*, 83–98.
- Bird, D. (2001), Shear margins: Continent-ocean transform and fracture zone boundaries, *Lead. Edge*, *20*(2), 150–159.
- Branch, T., O. Ritter, U. Weckmann, R. F. Sachsenhofer, and F. Schilling (2007), The Whitehill Formation—a high conductivity marker horizon in the Karoo Basin, *S. Afr. J. Geol.*, *110*(2/3), 465–476.
- Broad, D. S., E. H. A. Jungslager, I. R. McLachlan, and J. Roux (2006), Geology of the offshore Mesozoic basins, in *The Geology of South Africa*, edited by M. R. Johnson, C. R. Anhaeusser, and R. J. Thomas, pp. 553–571, Geol. Soc. of South Africa/Council for Geoscience, Pretoria, South Africa.
- Broquet, C. A. M. (1992), The sedimentary record of the Cape Supergroup: A review, in *Inversion Tectonics of the Cape Fold Belt, Karoo and Cretaceous Basins of Southern Africa*, edited by M. J. de Wit and I. G. D. Ransome, pp. 159–183, A.A. Balkema, Brookfield, Vt.
- Catuneanu, O., P. J. Hancox, and B. S. Rubidge (1998), Reciprocal flexural behaviour and contrasting stratigraphies: A new basin development model for the Karoo retroarc foreland system, South Africa, *Basin Res.*, *10*, 417–439.
- Christensen, N. I., and W. D. Mooney (1995), Seismic velocity structure and composition of the continental crust: A global view, *J. Geophys. Res.*, *100*(B6), 9761–9788.
- Cloetingh, S., A. Lankreijer, M. J. de Wit, and I. Martinez (1992), Subsidence history analyses and forward modelling of the Cape and Karoo Supergroups, in *Inversion Tectonics of the Cape Fold Belt, Karoo and Cretaceous Basins of Southern Africa*, edited by M. J. de Wit and I. G. D. Ransome, pp. 239–248, A.A. Balkema, Rotterdam, Netherlands.
- Cole, D. I. (1992), Evolution and development of the Karoo Basin, in *Inversion Tectonics of the Cape Fold Belt, Karoo and Cretaceous Basins of Southern Africa*, edited by M. J. de Wit and I. G. D. Ransome, pp. 87–99, A.A. Balkema, Rotterdam, Netherlands.
- de Beer, J. H., and D. I. Gough (1980), Conductive structures in southernmost Africa: A magnetometer array study, *Geophys. J. R. Astron. Soc.*, *63*, 479–495.
- de Beer, J. H., J. S. V. Van Zyl, and F. K. Bahnmann (1974), Plate tectonic origin for the Cape Fold Belt?, *Nature*, *252*, 675–676.
- Dewey, J. F., L. Robb, and L. van Schalkwyk (2006), Did Bushmanland extensionally unroof Namaqualand, *Precambrian Res.*, *150*, 173–182.
- de Wit, M. J. (1992), The Cape Fold Belt: A challenge for an integrated approach to inversion tectonics, in *Inversion Tectonics of the Cape Fold Belt, Karoo and Cretaceous Basins of Southern Africa*, edited by M. J. de Wit and I. G. D. Ransome, pp. 3–12, A.A. Balkema, Rotterdam, Netherlands.
- de Wit, M. J. (2007), The Kalahari Epeirogeny and climate change: Differentiating cause and effect from core to space, *S. Afr. J. Geol.*, *110*(2/3), 367–392.
- de Wit, M. J., and B. Horsfield (2006), Inkaba yeAfrica Project surveys sector of Earth from core to space, *Eos Trans. AGU*, *87*(11), 113, doi:10.1029/2006EO110002.
- Durrheim, R. J. (1987), Seismic reflection and refraction studies of the deep structure of the Agulhas Bank, *Geophys. J. R. Astron. Soc.*, *89*, 395–398.
- Durrheim, R. J., and W. D. Mooney (1994), Evolution of the Precambrian lithosphere: Seismological and geochemical constraints, *J. Geophys. Res.*, *99*(B8), 15,359–15,374.
- Eglinton, B. M. (2006), Evolution of the Namaqua-Natal Belt, southern Africa—A geochronological and isotope geochemical review, *J. Afr. Earth Sci.*, *46*, 93–111.
- Eglinton, B. M., and R. A. Armstrong (2003), Geochronological and isotopic constraints on the Mesoproterozoic Namaqua-Natal Belt: Evidence from deep borehole intersections in South Africa, *Precambrian Res.*, *125*, 179–189.
- Fouche, J., K. J. Bate, and R. van der Merwe (1992), Plate tectonic setting of the Mesozoic Basins, southern offshore, South Africa: A review, in *Inversion Tectonics of the Cape Fold Belt, Karoo and Cretaceous Basins of Southern Africa*, edited by M. J. de Wit and I. G. D. Ransome, pp. 27–32, A.A. Balkema, Rotterdam, Netherlands.

- Gernigon, L., J.-C. Ringenbach, S. Planke, and B. Le Gall (2004), Deep structures and breakup along volcanic rifted margins: Insights from integrated studies along the outer Vøring Basin (Norway), *Mar. Pet. Geol.*, *21*, 363–372.
- Gough, D. I. (1973), Possible linear plume under southernmost Africa, *Nat. Phys. Sci.*, *245*, 93–94.
- Gough, D. I., J. H. de Beer, and J. S. V. Van Zyl (1973), A magnetometer array study in southern Africa, *Geophys. J. R. Astron. Soc.*, *34*, 421–433.
- Green, R. W. E., and R. J. Durrheim (1990), A seismic refraction investigation of the Namaqualand metamorphic complex, South Africa, *J. Geophys. Res.*, *95*(B12), 19,927–19,932.
- Hälbich, I. W. (1983), A tectogenesis of the Cape Fold Belt (CFB), in *Geodynamics of the Cape Fold Belt*, edited by A. P. G. Söhnge and I. W. Hälbich, pp. 165–175, Special Publication of the Geol. Soc. of South Africa.
- Hälbich, I. W. (1993), The Cape Fold Belt—Aguilhas Bank Transect across the Gondwana Suture in southern Africa, in *American Geophysical Union Special Publication*, vol. 202, 18 pp., AGU Press, Washington, D.C.
- Hälbich, I. W., and J. Swart (1983), Structural zoning and dynamic history of the cover rocks of the Cape Fold Belt, in *Geodynamics of the Cape Fold Belt*, edited by A. P. G. Söhnge and I. W. Hälbich, Special Publication, pp. 75–100, Geological Society of South Africa, Johannesburg, South Africa.
- Harvey, J. D., M. J. de Wit, J. Stankiewicz, and C. M. Doucoure (2001), Structural variations of the crust in the Southwestern Cape, deduced from seismic receiver functions, *S. Afr. J. Geol.*, *104*, 231–242.
- Hirsch, K. K., K. Bauer, and M. Scheck-Wenderoth (2008), Deep structure of the western South African passive margin—Results of a combined approach of seismic, gravity and isostatic investigations, *Tectonophysics*, doi:10.1016/j.tecto.2008.04.028.
- Jacobs, J., and R. J. Thomas (1994), Oblique collision at 1.1 Ga along the southern margin of the Kaapvaal continent, SE Africa, *Geol. Rundsch.*, *83*, 322–333.
- Jacobs, J., R. J. Thomas, and K. Weber (1993), Accretion and indentation tectonics at the southern edge of the Kaapvaal craton during the Kibaran (Grenville) orogeny, *Geology*, *21*, 203–206.
- Lindeque, A. S., T. Ryberg, J. Stankiewicz, M. Weber, and M. J. de Wit (2007), Deep crustal seismic reflection experiment across the southern Karoo Basin, South Africa, *S. Afr. J. Geol.*, *110*(2/3), 419–438.
- Martin, A. K., C. J. H. Hartnady, and S. W. Goodland (1981), A revised fit of South America and South Central Africa, *Earth Planet. Sci. Lett.*, *75*, 293–305.
- McCourt, S., R. A. Armstrong, G. H. Grantham, and R. J. Thomas (2006), Geology and evolution of the Natal Belt, South Africa, *J. Afr. Earth Sci.*, *46*, 71–92.
- McMillan, I. K., G. I. Brink, D. S. Broad, and J. J. Maier (1997), Late Mesozoic basins off the south coast of South Africa, in *African Basins*, edited by R. C. Selley, pp. 319–376, Elsevier, New York.
- Menzies, M. A., S. L. Klempner, C. J. Ebinger, and J. Baker (2002), Characteristics of volcanic rifted margins, in *Volcanic Rifted Margins*, *GSA Special Paper*, vol. 362, edited by M. A. Menzies et al., pp. 1–14, Geological Society of America, Boulder, Colorado.
- Nair, S. K., S. S. Gao, K. H. Liu, and P. G. Silver (2006), Southern Africa crustal evolution and composition: Constraints from receiver function studies, *J. Geophys. Res.*, *111*, B02304, doi:10.1029/2005JB003802.
- Newton, A. R. (1992), Thrusting on the northern margin of the Cape Fold Belt, near Laingsburg, in *Inversion Tectonics of the Cape Fold Belt, Karoo and Cretaceous Basins of Southern Africa*, edited by M. J. de Wit and I. G. D. Ransome, pp. 193–196, A.A. Balkema, Rotterdam, Netherlands.
- Nguuri, T. K., J. Gore, D. E. James, S. J. Webb, C. Wright, T. G. Zengeni, O. Gwavava, J. Snoko and Kaapvaal Seismic Group (2001), Crustal structure beneath southern Africa and its implications for the formation and evolution of the Kaapvaal and Zimbabwe cratons, *Geophys. Res. Lett.*, *28*(13), 2501–2504.
- Oguti, J. (1964), Geomagnetic anomaly around the continental shelf margin southern offshore of Africa, *J. Geomagn. Geoelectr.*, *16*, 65–67.
- Parsiegla, N., K. Gohl, and G. Uenzelmann-Neben (2007), Deep crustal structure of the sheared South African continental margin: First results of the Agulhas-Karoo geoscience transect, *S. Afr. J. Geol.*, *110*(2/3), 393–406.
- Parsiegla, N., K. Gohl, and G. Uenzelmann-Neben (2008), The Agulhas Plateau: Structure and evolution of a large igneous province, *Geophys. J. Int.*, *174*, 336–350, doi:10.1111/j.1365-1246X.2008.03808.x.
- Paton, D. A., D. I. M. Macdonald, and J. R. Underhill (2006), Applicability of thin or thick skinned structural models in a region of multiple inversion episodes; southern South Africa, *J. Struct. Geol.*, *28*, 1933–1947.
- Pitts, B., M. Maher, J. H. de Beer, and D. I. Gough (1992), Interpretation of magnetic, gravity and magnetotelluric data across the Cape Fold Belt and Karoo Basin, in *Inversion Tectonics of the Cape Fold Belt, Karoo and Cretaceous Basins of Southern Africa*, edited by M. J. de Wit and I. G. D. Ransome, pp. 33–45, A.A. Balkema, Rotterdam, Netherlands.
- Rabinowitz, P. D., and J. LaBrecque (1979), The Mesozoic South Atlantic Ocean and evolution of its continental margins, *J. Geophys. Res.*, *84*(B11), 5973–6002.
- Raith, J. G., D. H. Cornell, H. E. Frimmel, and C. H. de Beer (2003), New insights into the geology of the Namaqua tectonic province, South Africa, from ion probe dating of detrital and metamorphic zircons, *J. Geol.*, *111*, 347–366.
- Robb, L. J., R. A. Armstrong, and D. J. Waters (1999), The history of granulite-facies metamorphism and crustal growth from single zircon U-Pb geochronology: Namaqualand, South Africa, *J. Petrol.*, *40*, 1747–1770.
- Ryberg, T., M. Weber, Z. Garfunkel, and Y. Bartov (2007), The shallow velocity structure across the Dead Sea Transform fault, Arava Valley, from seismic data, *J. Geophys. Res.*, *112*, B08307, doi:10.1029/2006JB004563.
- Schmitz, M. D., and S. A. Bowring (2004), Lower crustal granulite formation during Mesoproterozoic Namaqua-Natal collisional orogenesis, southern Africa, *S. Afr. J. Geol.*, *107*, 261–284.
- Scrutton, R. A., and A. du Plessis (1973), Possible marginal fracture ridge south of South Africa, *Nature*, *242*, 180–182.
- Stankiewicz, J., T. Ryberg, A. Schulze, A. S. Lindeque, M. Weber, and M. J. de Wit (2007), Initial results from wide-angle seismic refraction lines in the Southern Cape, *S. Afr. J. Geol.*, *110*(2/3), 407–418.
- Talwani, M., and O. Eldholm (1973), The boundary between continental and oceanic basement at the margin of rifted continents, *Nature*, *241*, 325–330.
- Tankard, A. J., M. P. A. Jackson, K. A. Eriksson, D. K. Hobday, D. R. Hunter, and W. E. L. Minter (1982), *Crustal Evolution of Southern Africa*, Springer, New York.
- Thomson, K. (1999), Role of the continental break-up, mantle plume development and fault activation in the evolution of the Gamtoos Basin, South Africa, *Mar. Pet. Geol.*, *16*, 409–429.
- Trumbull, R. B., S. V. Sobolev, and K. Bauer (2002), Petrophysical modelling of high seismic velocity crust at the Namibian volcanic margin, in *Volcanic Rifted Margins*, *GSA Special Paper*, vol. 362, edited by M. A. Menzies et al., pp. 221–230, Geological Society of America, Boulder, Colorado.
- Trumbull, R. B., D. L. Reid, C. H. De Beer, and R. L. Romer (2007), Magmatism and continental breakup at the west margin of southern Africa: A geochemical comparison of dolerite dikes from NW Namibia and the Western Cape, *S. Afr. J. Geol.*, *110*(2/3), 477–502.
- Uenzelmann-Neben, G., K. Gohl, A. Ehrhardt, and M. Seargent (1999), Agulhas Plateau, SW Indian Ocean: New evidence for excessive volcanism, *Geophys. Res. Lett.*, *26*(13), 1941–1944.
- Vidale, J. E. (1988), Finite-difference calculation of travel times, *Bull. Seismol. Soc. Am.*, *78*(6), 2062–2076.
- Weckmann, U., O. Ritter, A. Jung, T. Branch, and M. J. de Wit (2007a), Magnetotelluric measurements across the Beattie magnetic anomaly and the Southern Cape Conductive Belt, South Africa, *J. Geophys. Res.*, *112*, B05416, doi:10.1029/2005JB003975.
- Weckmann, U., A. Jung, T. Branch, and O. Ritter (2007b), Comparison of electrical conductivity structures and 2D magnetic modelling along two profiles crossing the Beattie magnetic anomaly, South Africa, *S. Afr. J. Geol.*, *110*(2/3), 449–464.
- White, R. S., D. McKenzie, and R. K. O'Nions (1992), Oceanic crustal thickness from seismic measurements and rare Earth element inversions, *J. Geophys. Res.*, *97*(B13), 19,683–19,715.
- Zelt, C. A., and P. J. Barton (1998), Three-dimensional seismic refraction tomography: A comparison of two methods applied to data from the Faeroe Basin, *J. Geophys. Res.*, *103*(B4), 7187–7210.
- Zelt, C. A., and D. A. Forsyth (1994), Modelling wide-angle seismic data for crustal structure: Southeastern Grenville Province, *J. Geophys. Res.*, *99*(B6), 11,687–11,704.
- Zelt, C. A., and R. B. Smith (1992), Seismic traveltime inversion for 2-D crustal velocity structure, *Geophys. J. Int.*, *108*, 16–34.

K. Gohl and N. Parsiegla, Alfred Wegener Institute for Polar and Marine Research, P.O. Box 12161, 27515, Bremerhaven, Germany.

T. Ryberg, J. Stankiewicz, R. Trumbull, M. Weber, and U. Weckmann, GeoForschungsZentrum Potsdam, Section 2.2 (Deep Geophysical Sounding), Telegrafenberg, Potsdam, Brandenburg 14473, Germany. (jacek@gfz-potsdam.de)